OPTIMUM CORE-WINDING RATIO FOR A RECEIVER COIL IN A BIOMEDICAL INDUCTIVE POWER SYSTEM

Furqan Noor[1] and Maeve Duffy[2]
[1]*Bioelectronics Research Cluster, National University of Ireland Galway, Galway, Ireland*
[2]*Power Electronics Research Centre, National University of Ireland Galway, Galway, Ireland*

Keywords: Biomedical inductive power systems, Transplants, coils, Maximum power transfer, Magnetic cores.

Abstract: The relation of the structure of a cylindrical coil used on the receiver side of an inductive power system to the level of power that can be delivered is investigated. It is found that for a given fixed receiver coil size, an optimum design can be defined in which the cross sectional area of the core equals that of the winding. Results of circuit simulation, Finite Element Analysis and measurements of five test coils are presented to verify the proposed theory for the case of coils having 5 mm diameter and 10 mm length.

SCIENCE AND TECHNOLOGY PUBLICATIONS

1 INTRODUCTION

Wireless power links have been widely applied in biomedical applications, for their advantages of reduced infection, reduced size and simplified or reduced surgical procedures. However, in proven systems it is generally true that power transmitter and receiver coils are located in close proximity and the power requirements are relatively low (Clements, Vichienchom et al. 1999; Ahmadian, Flynn et al. 2005; Atluri and Ghovanloo 2005; Fotopoulou and Flynn 2006; Harrison, Watkins et al. 2006; Ali, Ahmad et al. 2009). Furthermore, most of the biomedical inductive power transfer (IPT) systems developed so far do not have such strict constraints of physical dimensions of the transmitter and receiver coils and the spacing between them (Clements, Vichienchom et al. 1999; Atluri and Ghovanloo 2005; Hmida, Dhieb et al. 2006; Furse, Harrison et al. 2007; Mounaim, Sawan et al. 2009). In this work, transmitter and receiver coils that have significantly different sizes (50 mm vs. 5 mm diameter), and which are located at a large distance apart (when compared to the size of the received coil) are investigated. Both primary and receiver coils are assumed to be located inside the body, with the battery powered transmitter coil located so that it can provide power to a receiver coil located in a more inaccessible part of the body.

Initially, the case of air-core coils was investigated, but it was found that low coupling between transmitter and receiver coils seriously limits the power transfer capability. The inclusion of a magnetic core in the receiver coil was found to enhance the power transfer efficiency by increasing the mutual coupling between the coils (Noor and Duffy 2009). Cores have been used in the receiver coils of biomedical applications like BION implants (J. H. Schulman 2004; Djordje Popovic 2007), biomedical sensors (Flynn), and wireless powering of implantable devices (Kihyun Jung 2008). However, no detail is available on how the design of receiver coils with cores should be optimised, and therefore this work addresses this issue.

The design and construction of 5 test receiver coils for a given air-core transmitter coil is described in section 2. Resonant circuits used to compensate for the high leakage inductance associated with a loosely coupled system are described in section 3. The design of a suitable resonant circuit in terms of the inductances, resistances and coupling factor for a given pair of transmitter and receiver coils is described so that the results can be investigated for other systems. Results of power and voltage levels are predicted for the five test coils over frequencies from 100 – 600 kHz. It is found that the maximum power is provided with a coil in which the core and winding cross sectional areas are approximately equal, where the increase in coupling factor provided by the core is offset by the reduction in winding turns that can be fit for larger core areas. The translation of power levels achieved in terms of electromagnetic field regulations for safe human

Noor F. and Duffy M..
OPTIMUM CORE-WINDING RATIO FOR A RECEIVER COIL IN A BIOMEDICAL INDUCTIVE POWER SYSTEM.
DOI: 10.5220/0003169500740086
In *Proceedings of the International Conference on Biomedical Electronics and Devices* (BIODEVICES-2011), pages 74-86
ISBN: 978-989-8425-37-9
Copyright © 2011 SCITEPRESS (Science and Technology Publications, Lda.)

exposure (IEEEStandard 1999) is discussed in section 4. Both cases of continuous and pulsed powering are considered. Finally, measurement results of power and voltage produced for the test coils are presented in section 5, where it is shown that continuous power levels of up to 3.6 μW can be provided within the electromagnetic field regulations, thereby also confirming predicted pulse power levels of up to 12 mW.

2 TRANSMITTER & RECEIVER COILS

It was previously confirmed that the placement of a magnetic core in the receiver coil of the inductive power system provides amplification in the power transfer (Noor and Duffy 2009). The application of ferrite rod cores is investigated in this paper, where the main aim is to identify an optimum core-winding combination for the receiver coil that maximizes power delivery to the load within the electromagnetic field regulations. In all cases, a transmitter coil with outer diameter of 51 mm and N_{tx} = 10 turns is assumed; practically the coil was wound using wire with a diameter, d_{wtx}, of 0.5 mm over an axial length of 5 mm.

Power available from a receiver coil in an inductive power system is proportional to the square of the voltage induced on it, $V_{ind}^2 = (j\omega MI_{tx})^2$, and inversely proportional to the coil resistance, R_2, where M is the mutual inductance between the transmitter and receiver coils and I_{tx} is current flowing in the transmitter coil. In terms of a cylindrical receiver coil with a rod shaped core, the induced voltage may be given as:

$$V_{ind} = j\omega N_{rx} \pi CD^2 B / 4 \quad (1)$$

where N_{rx} is the number of receiver turns, CD is the diameter of the core and B is the magnetic flux density established in the area of the core for a given transmitter current, I_{tx}. Similarly, the DC resistance of the coil can be given in terms of the physical parameters of the winding as:

$$R_2 = \frac{\rho N_{rx} \pi (OD + CD)/2}{\pi d_{wrx}{}^2 / 4} \quad (2)$$

Where ρ is the resistivity of the coil wire, OD is the outer diameter of the coil and d_{wrx} is the wire diameter. Combining (1) and (2), a relationship between the available output power, P_{avail}, and the coil parameters is found as:

$$P_{avail} \propto \frac{(\omega N_{rx} CD^2 B)^2 d_{wrx}{}^2}{\rho N_{rx} (OD + CD)} \quad (3)$$

For the purpose of comparing different receiver coil geometries, it is assumed that ω, d_{wrx}, B and ρ are all constant. Furthermore, the coils are compared for a fixed outer coil diameter, OD, and a fixed coil length. Finally, recognising that there is a proportional relationship between the number of winding turns and the space available in a given winding width, (OD – CD)/2, (3) can be expressed entirely in terms of the coil radial dimensions:

$$P_{avail} \propto \frac{(OD - CD) CD^4}{(OD + CD)} \quad (4)$$

Differentiating P_{avail} in terms of CD, the condition for an optimum receiver coil design is identified as:

$$CD = 0.781\ OD \quad (5)$$

Further investigation confirms that this condition is approximately the same as found by equating the cross sectional areas of the core, $\pi CD^2/4$, and the winding, $\pi(OD^2 - CD^2)/4$; i.e. there is a trade off between the number of winding turns that can be fit and the flux linkage area provided by the core.

In order to confirm this theory, wire with a diameter, d_{wrx} = 0.16 mm, was used to wind five receiver coils over a length, l_{rx}, of 10 mm. The coils were wound on five different ferrite rod cores with diameter, CD, varying from 4 mm to 1.5 mm. All windings were wound to produce an overall coil diameter OD = 5 mm. The corresponding number of turns, N_{rx}, ranges from 106 to 330 respectively. The core material has an initial magnetic permeability of 2300 (fair-rite) in all cases. A cross section of the coils is shown in Figure 1 and a photograph of the transmitter and receiver coils is shown in Figure 2.

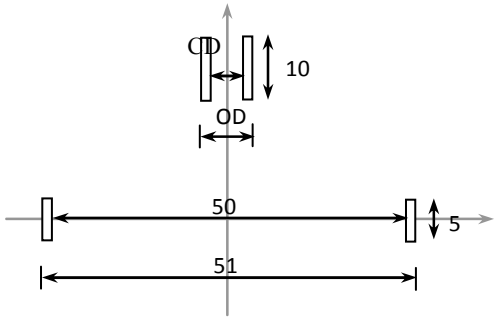

Figure 1: Cross section of test transmitter and receiver coils. (Dimensions in mm, not to scale).

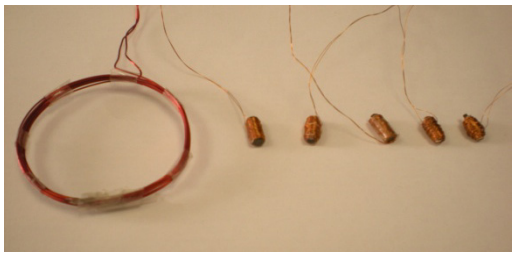

Figure 2: Transmitter Coil (large) with 5 (small) receiver coils of different turn-core ratio.

The core dimensions and turns specifications of the five receiver coils are compared in Table 1, along with predicted and measured inductance values. Predicted values L_{FEA}, were found using Finite Element Analysis (FEA) (Maxwell2d), and measurements, L_{meas}, were performed using an impedance analyser (Agilent 4395A). Results of DC winding resistance and coupling factor, k, are also included in Table I, where FEA modelling was used to predict k between transmitter and receiver coils when separated by an axial distance of 5.5 cm.

Table 1: Receiver Coils' Specifications.

Coil #	1	2	3	4	5
CD	4	3	2.5	2	1.5
N	106	208	231	285	330
L_{FEA} (μH)	134	410	430	800	590
L_{meas} (μH) @ 200 kHz	146	425	420	873	396
R_{DC}(Ω)	2.5	3.8	4.2	4.4	4.8
k	0.0041	0.0032	0.0031	0.0027	0.0025

There is generally agreement among the two methods used for determining receiver coil inductance, L_2. Predicted values are generally higher and this may be explained by the tolerance of the core permeability and by the difference between modelled and practical winding dimensions. As might be expected, coupling factor increases with increasing core diameter. These values will be compared with measurements later in section 3.

3 RESONANT CIRCUIT DESIGN

In order to investigate the maximum power transfer capability of an inductive link it is necessary to determine the relationship between different circuit parameters. These expressions eventually lead to an optimum load resistance for a given coil operating at a given frequency. In the case of links with low coupling it is found that it's more appropriate to first aim for a maximum level of power transfer, and then to try to optimize for maximum efficiency.

The impedance of the receiver leakage inductance is quite large at weak coupling, and therefore requires a high induced voltage on the receiver coil. This in turn requires high transmitter coil voltage and current and thus induces losses and depreciates the efficiency of the inductive link. In order to cancel the leakage inductance, the receiver coil can be compensated by a series or parallel capacitor. This process induces resonance in the receiver circuit and the link operates at the phase resonance frequency of the receiver coil. As a result, real power transmission can be increased while keeping the product of voltage and current (VA) requirements low. A parallel compensated receiver coil as shown in Figure 3 acts as a current source and is usually preferred as the controllability of the design is straight forward by employing short circuit control (Stielau and Covic 2000). A receiver coil can also be compensated by a series capacitor.

Compensation of the transmitter coil is also essential to compensate not only the transmitter coil inductance but also any reflected impedance from the receiver; this is particularly important if there is a lot of variation in the inductive parameters of the system due to deformation or movement of the coils. Just like the receiver coil, the transmitter coil can also be compensated with a series or parallel capacitor.

3.1 Circuit Analysis

An inductive link with both coils compensated using parallel capacitors as in Figure 3 is analyzed to determine an expression for maximum power transfer in terms of the electrical parameters of the transmitter and receiver coils The total impedance acting against the voltage induced on the receiver side, Z_2, can be written as:

$$Z_2 = R_2 + j\omega L_2 + \frac{\frac{R_L}{j\omega C_2}}{R_L + \frac{1}{j\omega C_2}} \quad (6)$$

At the receiver resonant frequency the imaginary component of Z_2 becomes zero, thereby defining the resonant frequency, ω_0, as:

$$\omega_0 = \sqrt{\frac{1}{L_2 C_2} - \frac{1}{(C_2 R_L)^2}} \quad (7)$$

Thus at resonance the total impedance of the receiver side of the circuit is real and Z_2 can be written as

$$Z_2 = R_2 + \frac{R_L}{(\omega_0 C_2 R_L)^2} \quad (8)$$

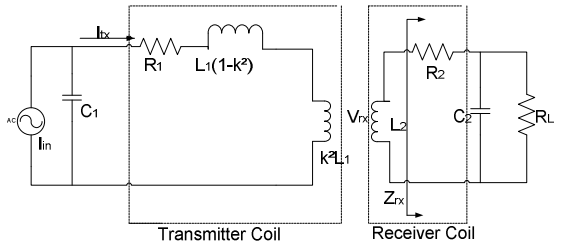

Figure 3: Transformer model of a parallel compensated inductive power system.

For simplicity, the impedance presented at the terminals of the transmitter coil in Figure 3 can be given in terms of the impedance of the receiver circuit referred to the transmitter side as shown in Figure 4 (Schuylenbergh 1999), where Z_{ref} is Z_{rx} referred to the transmitter side:

$$Z_{ref} = (\frac{k}{n})^2 Z_{rx} \quad \text{with} \quad n = \sqrt{\frac{L_1}{L_2}} \quad (9)$$

and Z_{rx}, is the impedance of the receiver circuit other than the coil self inductance L_2.

$$Z_{rx} = R_2 + \frac{R_L}{1 + j\omega C_2 R_L} \quad (10)$$

The transmitter circuit model can be further reduced to an equivalent impedance Z_{tot} acting in series with the primary coil inductance L_1 as shown in Figure 4.

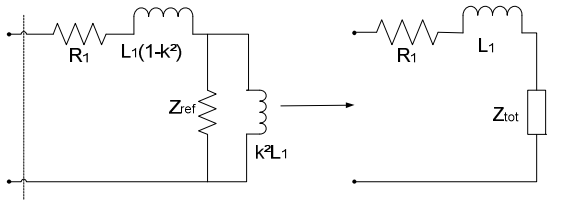

Figure 4: Simplified transmitter coil circuit.

At the receiver resonant frequency, it is found that Z_{tot} is a real quantity which can be defined as R_{tot} given by:

$$R_{tot} = \frac{k^2 L_1 (C_2 R_L^2 - L_2)}{C_2 R_L (C_2 R_L R_2 + L_2)} \quad (11)$$

Therefore, at resonance, the primary link efficiency can be written as

$$\eta_{tx} = \frac{R_{tot}}{R_{tot} + R_1} \quad (12)$$

which is given in terms of the circuit components by substituting (11) into (12):

$$\eta_{tx} = \frac{(k^2 L_1)(C_2 R_L^2 - L_2)}{(k^2 L_1)(C_2 R_L^2 - L_2) + C_2 R_L R_1 (C_2 R_L R_2 + L_2)} \quad (13)$$

Note that this expression holds true regardless of whether or not a resonant capacitor, C_1, is included on the transmitter side. In most practical systems however, a resonant capacitor is included so that a lower source voltage can be applied. For loosely coupled systems, it is found that C_1 is given simply in terms of the transmitter coil inductance and resonant frequency:

$$C_1 = \frac{1}{\omega_o^2 L_1} \quad (14)$$

The receiver link efficiency can be defined as the ratio of useful power dissipated in the equivalent ac load, P_L, to the power transmitted to the receiver circuit, P_{rx}.

$$\eta_{rx} = \frac{P_L}{P_{rx}} \quad (15)$$

In turn, load power may be given as:

$$P_L = \frac{|V_L|^2}{R_L}, \text{ with } V_L = \frac{V_{rx} Z_L}{R_2 + Z_L} \quad (16)$$

V_{rx} is the load voltage driving Z_{rx} across the ideal circuit model of the receiver coil, and Z_L is the parallel combination of R_L and C_2:

$$Z_L = -\frac{jR_L}{\omega C_2 R_L - j} \quad (17)$$

Substituting (17) into (16) the resulting expression for load voltage is given as:

$$V_L = \frac{V_{rx} R_L (R_2 + R_L + j\omega C_2 R_L R_2)}{(\omega C_2 R_L R_2)^2 + (R_2 + R_L)^2} \quad (18)$$

and the power delivered to the load resistor can be written as

$$P_L = \frac{V_{rx}^2 R_L}{(\omega C_2 R_L R_2)^2 + (R_2 + R_L)^2} \quad (19)$$

Similarly, the total power delivered to the receiver circuit can now be written in terms of V_{rx} as:

$$P_{rx} = P_L + \left|\frac{V_L}{Z_L}\right|^2 R_2 = P_L + \left|\frac{V_{rx}}{R_2 + Z_L}\right|^2 R_2 \quad (20)$$

SCITEPRESS SCIENCE AND TECHNOLOGY PUBLICATIONS

That is:

$$P_{rx} = \frac{V_{rx}^2[R_2(\omega C_2 R_L)^2 + (R_2 + R_L)]}{(\omega C_2 R_L R_2)^2 + (R_2 + R_L)^2} \quad (21)$$

Substituting for P_L and P_{rx} into (15), the efficiency of the receiver circuit can be determined as follows

$$\eta_{rx} = \frac{R_L}{R_2(\omega C_2 R_L)^2 + (R_2 + R_L)} \quad (22)$$

At the resonant frequency (22) reduces to

$$\eta_{rx} = \frac{L_2}{L_2 + C_2 R_L R_2} \quad (23)$$

And the total link efficiency is given by:

$$\eta_{link} = \eta_{tx}\eta_{rx} \quad (24)$$

Power transfer to the load is the product of the link efficiency and the total real power delivered by the driver of the transmitter coil:

$$P_L = \eta_{link} P_{tx} \quad (25)$$

Given that one limitation to the power level that can be transmitted in biomedical applications is the maximum magnetic field intensity, H, that can be applied, it is convenient to express load power in terms of the transmitter current, I_{tx}, to which the H field is in direct proportion. More details of the H field limitation are given in section 4. At resonance, the total power delivered from the driver is given in terms of I_{tx} as:

$$P_{tx} = I_{tx}^2 (R_1 + R_{tot}) \quad (26)$$

where R_1 is the equivalent resistance of the transmitter coil. Substituting for R_{tot} from (11) the total power transfer to the load can be written as:

$$P_L = \frac{(k^2 L_1)(\omega_0 L_2)^2 C_2 R_L}{(L_2 + C_2 R_L R_2)^2} I_{tx}^2 \quad (27)$$

Clearly, power transfer is proportional to the square of the reactance of the receiver coil and of current flowing in the transmitter coil. This relationship is used to scale power levels according to the maximum current that can be applied within the field regulations for different transmitter coil excitation options in section 4.

Finally, the rms value of the load voltage at resonance, V_L, can be deduced as:

$$\frac{V_L^2}{R_L} = \frac{(k^2 L_1)(\omega_0 L_2)^2 C_2 R_L}{(L_2 + C_2 R_L R_2)^2} I_{tx}^2 \quad (28)$$

to give:

$$V_L = \frac{(\omega_0 L_2)\sqrt{(k^2 L_1)(C_2 R_L^2)}}{L_2 + C_2 R_L R_2} I_{tx} \quad (29)$$

Analysing (28), it is found that each receiver coil has an optimum load resistor, R_{Lopt}, at a given resonance frequency. This optimum value can be found by differentiating P_L with respect to R_L, where it is found that:

$$R_{Lopm} = \frac{L_2}{C_2 R_2} \quad (30)$$

Substituting for C_2 from (7), R_{Lopm} is defined entirely in terms of the receiver coil impedances:

$$R_{Lopm} = \frac{(\omega_0 L_2)^2 + R_2^2}{R_2} \quad (31)$$

Substituting (31) into (27), the expression for maximum power transfer to the optimum load is found as:

$$P_{Lopm} = \frac{(k^2 L_1)(\omega_0 L_2)^2}{4(L_2 R_2)} I_{tx}^2 \quad (32)$$

For illustration, the optimum load resistor is verifed for coil 2 (with a 3 mm core) resonating at 320 kHz with C2 = 470 pF and R2 measured as 23.6 Ω (at 320 kHz). Using (30), the optimum load resistor for maximum power transfer is predicted as 38.4 kΩ with measured values of L1 and L2. The graph of PL vs. RL predicted using (27) in Figure 5 verifies the maximum power transfer at the calculated load.

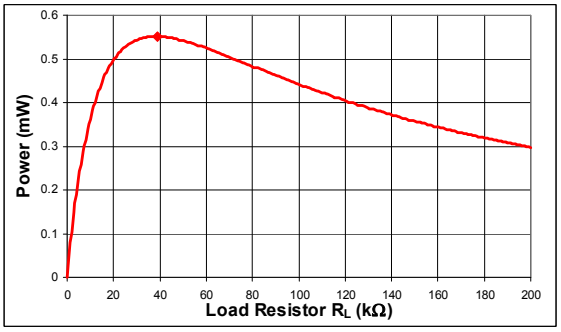

Figure 5: Maximum power transfer at optimum load.

3.2 Circuit Design for Given Transmitter and Receiver Coils

In order to enable a comparison of the different receiver coils under investigation, the circuit of Figure 3 was designed over a range of frequencies

SCITEPRESS
SCIENCE AND TECHNOLOGY PUBLICATIONS

(100 – 600 kHz) for each of the five test coils described in section 2. The main aim of circuit design is to determine the maximum power that can be transmitted to each coil for a given transmitter current, and the frequency at which this transfer occurs.

For each coil, the first step in design is to determine the resonant capacitance value, C_2, required for a given operating frequency, ω_0, using (7), with the optimum value of R_L determined from (31). For this purpose, values of R_2 and L_2 vs. frequency were measured using an impedance analyser so that their variation with frequency was accounted for. It was found that while inductance values remain practically constant with frequency, resistance values increase by up to one order of magnitude. This is explained by the combination of skin and proximity effects in the windings and the contribution of core losses from the ferrite rods, both of which are difficult to predict. Corresponding predicted results of R_{Lopm} are plotted vs. frequency for each of the 5 test coils in Figure 6.

The first thing to note is that R_{Lopm} increases with frequency for all coils. This is explained largely by increasing inductive impedance with frequency, and may be applied to tune a given system for maximum output power at a particular load resistance. The same effect applies in relation to the trends in R_{Lopm} predicted for different coils, where coil 4 has the largest inductance and coil 1 has the smallest.

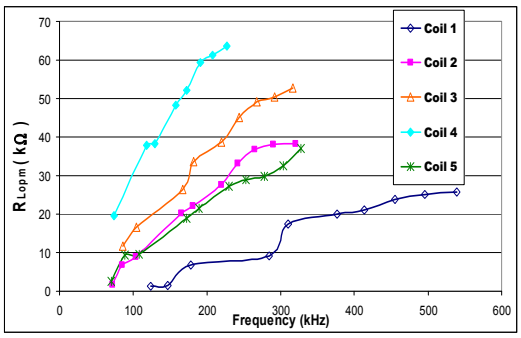

Figure 6: R_{Lopm} vs. frequency for the test receiver coils.

At this stage, the receiver circuit design is complete, and the only remaining parameter needed to complete circuit analysis is the coil coupling factor, k. This can be deduced from FEA models of the transmitter and coil structures. However, due to the large distance between the coils and the differences in their sizes in this case, it was found that the accuracy of FEA models is limited. As a second method, coupling factor was deduced from measurements of the voltage induced on the receiver coil. Due to the low level of these voltages, measurements needed to be performed under resonant conditions and this first required that the Q-factor of each coil be determined.

For a given receiver coil, the input voltage, V_{in}, applied to the series combination of the coil and its resonant capacitor, C_2, as shown in Figure 7 can be related to a larger valued output resonant voltage, V_{out}, to give the coil Q-factor. In this case, the resonant capacitor is given simply in terms of the resonant frequency, f_{res}, as:

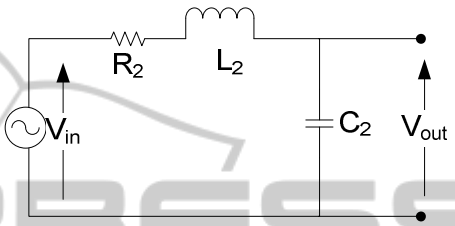

Figure 7: Setup for the measurement of Q_2.

$$C_2 = \frac{1}{(2\pi f_{res})^2 L_2} \tag{33}$$

V_{out} and V_{in} are then found to be related in terms of the Q-factor of the receiver coil, $Q_2 = \omega_o L_2/R_2 = 1/\omega_o C_2 R_2$:

$$V_{out} = -jV_{in}\frac{1}{\omega C_2 R_2} = -jQ_2 V_{in} \tag{34}$$

Using the function generator as a supply voltage, values of Q_2 were calculated using (34) for each of the test coils over a range of frequencies from 100 – 600 kHz. Values of coupling factor were then deduced from measurements of the voltage produced across the same resonant capacitor, V_{C2}, with the transmitter and receiver coils separated axially by 5.5 cm, and a given current, I_{tx}, supplied to the transmitter coil, as in the circuit of Figure 18. The voltage induced on the receiver coil V_{ind} was then calculated as:

$$V_{ind} = \frac{V_{C2}}{Q_2} \tag{35}$$

and the value of mutual inductance, M, between transmitter and receiver coils was found as:

$$M = \frac{V_{ind}}{j\omega I_{tx}} \tag{36}$$

Finally, the coupling factor k was calculated as:

$$k = \frac{M}{\sqrt{L_1 L_2}} \tag{37}$$

SCITEPRESS SCIENCE AND TECHNOLOGY PUBLICATIONS

using measured values of L_1 and L_2. The measured coupling factor for the five test coils is shown in Figure 8. Ideally, the coupling factors should not vary with frequency however; the measured values show a little variation because of the non ideal measurement conditions.

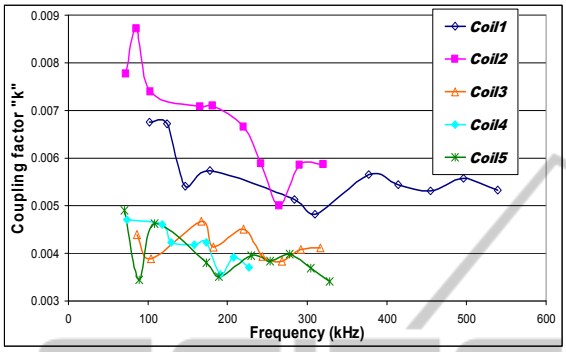

Figure 8: Measured coupling factors of test coils.

Coils 3, 4 and 5 have similar levels of coupling, all of which are lower than 0.005. The core area is smallest in these cases. It is interesting to note that when compared with FEA simulation, the maximum value of k is found with coil 2 rather than with coil 1 which has the largest core area. On further investigation, it is found that the core and winding cross sectional areas are approximately equal in coil 2, and this seems to confirm the optimum receiver structure identified in section 2, in which the reduction in core area is traded against an increasing number of turns. Work is ongoing to explain the difference in values of k deduced from FEA models and measurements.

3.3 Predicted Performance of Test Coils

Using (32), results of P_{Lopm} are predicted and plotted vs. frequency for each of the receiver coils at a transmitter coil current, I_{tx}, of 1 A in Figure 9. Corresponding values of V_{Lopm} are plotted in Figure 10. Note that these values correspond to the measured values of R_{Lopm} plotted in Figure 6. It is seen that as given by (32) and (31), both P_{Lopm} and V_{Lopm} increase with frequency, respectively. The factor of increase is lower than given by ω_o^2 and ω_0 respectively, due to the reduction in inductance and increase in resistance values with frequency.

Comparing P_{Lopm} for the different test coils, it is clear that coil 2 produces the highest power levels for most of the frequencies tested. This relates to coil 2 having the highest coupling factor as confirmed above and it supports the relationship to the core: winding ratio identified in section 2; i.e. the cross sectional areas of the core and winding are closest for coil 2. Coil 5 has the lowest power over all frequencies, and is most likely explained by its highest coil resistance due to the largest number of coil turns.

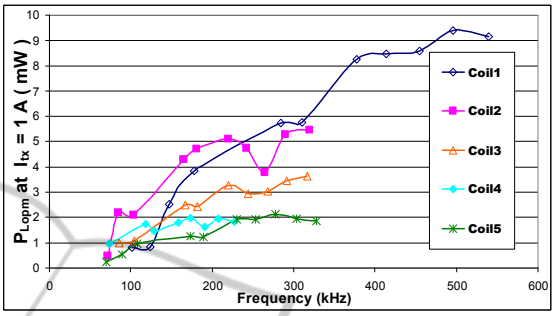

Figure 9: P_{Lmax} vs. frequency for the test receiver coils (I_{tx} = 1 A).

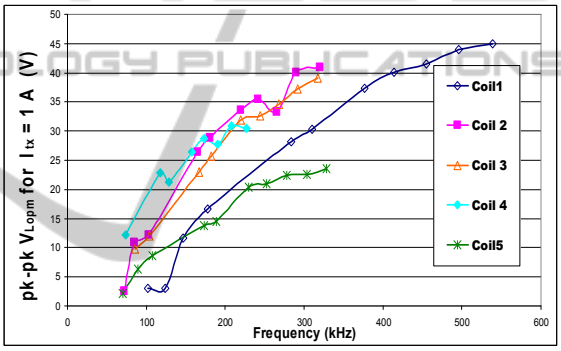

Figure 10: V_{Lopm} vs. frequency for the test receiver coils (I_{tx} = 1 A).

In relation to load voltages, coils 2, 3, and 4 produce similar levels, with the two extreme coil designs (having largest and smallest core areas) having the lowest levels. In this case the trend is explained approximately by the ratio of k/Q_2, so that the voltage of coil 1 is limited by high Q-factor and that of coil 5 is limited by low k.

These results are translated into power levels corresponding to the maximum transmitter current levels allowed according to the field regulations in section 4, and they are then verified by measurement in section 5.

4 IMPACT OF ELECTROMAGNETIC FIELD REGULATIONS

In biomedical applications there are restrictions

imposed by the ICNIRP for safe levels of electromagnetic fields for human exposure (IEEEStandard 1999). For a given set of inductive coils, this translates to a maximum transmitter coil current that must not be exceeded. Using this value of current, the question of how much power can be transmitted to a load connected on the receiver side without exceeding the electromagnetic field limitation is analyzed, to compare the performance of the different receiver coils under investigation. Results of voltage and power levels predicted in section 3 are scaled in terms of I_{tx} for this purpose.

Magnetic field intensity, H, at a distance of 2 mm from the transmitter coil is considered as a measure of the safe level of electromagnetic fields for human exposure. As shown in Figure 11, the 2 mm distance represents a box containing the transmitter coil and relevant circuitry, and so this is the H field that will be exposed to the body tissues.

The allowed limit for occupational exposure to magnetic field intensity for frequencies between .065 - 1 MHz is 1.6/f (f in MHz); i.e. the maximum allowed field intensity decreases with increasing frequency. Therefore, for an operating frequency of 260 kHz for example, the rms H field is limited to only 6.15 A/m. This H-field limit holds true for continuous sinusoidal current, or for any other waveform that produces the same rms current over a 6 minute interval (IEEEStandard 1999).

4.1 Continuous Powering

From FEA, it is deduced that a sinusoidal rms current of 1 A in the test ten turn transmitter coil corresponds a maximum rms H field, $H_{max(1A)}$, of 420 A/m at an axial distance of 2 mm from the coil. As magnetic field intensity is proportional to current in the transmitter coil, it is calculated for example that the maximum allowed rms transmitter current, $I_{tx(reg)}$, corresponding to a H-field limit, H_{reg}, of 6.15 A/m at 260 kHz is 15 mA using:

$$I_{tx(reg)} = \frac{H_{reg}}{H_{max(1A)}} \tag{38}$$

The corresponding maximum continuous power that can be transmitted to the load is then given by (32) with $I_{tx} = I_{tx(reg)}$.

For the given 10 turn transmitter coil, results of $I_{tx(reg)}$ are calculated using (38) for frequencies ranging from 100 – 600 kHz, with H_{reg} calculated as 1.6/f (f in MHz). Clearly, $I_{tx(reg)}$ decreases with frequency in the same way as H_{reg}. Equation (32) is then applied to predict the corresponding maximum power levels possible, as given in Figure 12, where the system is designed according to the procedure described in section 3.3. In effect, the results of Figure 12 are scaled versions of those given in Figure 9 according to $I_{tx(reg)}^2$. Corresponding values of pk-pk voltage are presented in Figure 13.

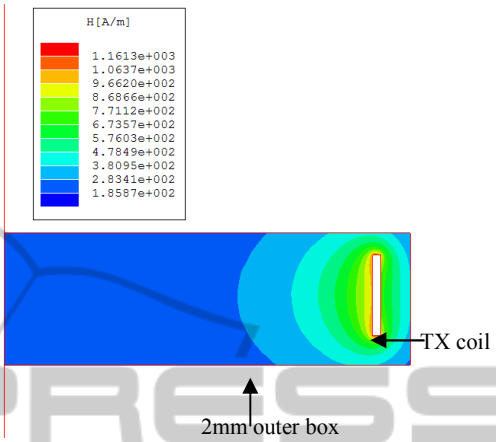

Figure 11: Magnetic field intensity around the transmitter coil for a current of 1 A rms.

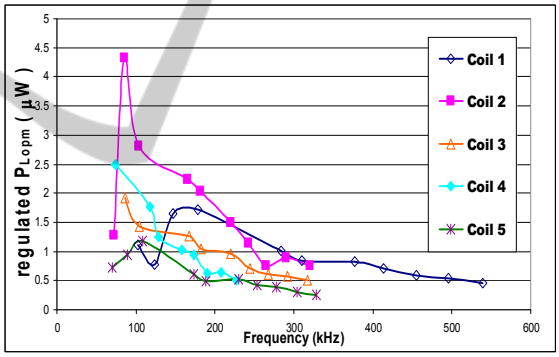

Figure 12: Predicted maximum continuous power within field limitations.

In the same way as in Figure 9, coil 2 provides the highest output power when Itx is limited according to electromagnetic regulations. A mximum power level of 4.3 μW is predicted at 100 kHz. Due to the allowance for higher currents at lower frequencies, it is seen that the relative performance of coil 2 is enhanced over all other coils, and it provides the maximum power over all frequencies considered. Trends in pk-pk voltage levels in Figure 13 are similar to those presented in Figure 10 , with a pk-pk voltage of 0.5 V achieved for the maximum power point of coil 2.

SCITEPRESS SCIENCE AND TECHNOLOGY PUBLICATIONS

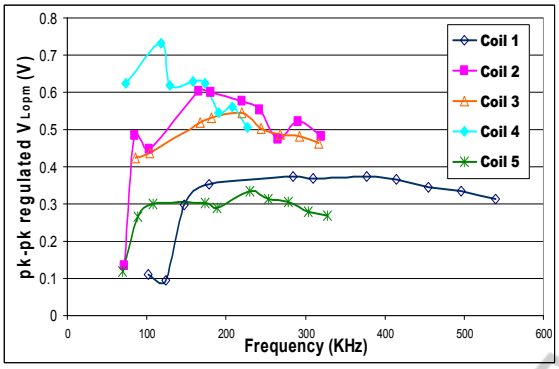

Figure 13: Predicted pk-pk load voltage within field limitations.

4.2 Pulse Powering

In biomedical applications, power is often required in short bursts of time over a longer repetitive period. Therefore, it is possible to provide power through an inductive link by driving high current in the transmitter coil for short intervals of time. The maximum value of allowed current in the transmitter coil is a function of the repetition frequency, f = 1/T, and the width of the pulse, PW, used. The maximum allowed sinusoidal H field amplitude, $H_{pk(reg)}$, applied during the pulse time, PW, can be calculated in terms of its rms value as:

$$\sqrt{\frac{H_{pk}^{2}.PW}{2T}} = H_{reg} \qquad (39)$$

The maximum instantaneous transmitter peak current, $I_{pk(reg)}$, is proportional to $H_{pk(reg)}$ as before. For an rms current of 1 A the simulated rms H field is 425 A/m as described earlier; thus the allowed peak current amplitude can be scaled as:

$$I_{pk(reg)} = \frac{H_{pk(reg)}}{425} \qquad (40)$$

The corresponding peak instantaneous power that can be transmitted during pulsed operation can then be calculated using (32) with $I_{tx} = I_{pk(reg)}$. The performance of the five test coils for pulse durations of 0.5 ms and 1 ms is shown in Figures 14, 15, 16 and 17 in terms of the maximum instantaneous power levels and the maximum pk-pk load voltages. The time period used for pulse powering is 0.833 seconds in all cases.

As in the case of continuous powering, there is an optimum frequency at which the maximum instantaneous power occurs for every test coil. Obviously, instantaneous pulse power and voltage levels are significantly higher than corresponding average values (shown in Figure 12 and 13), and the levels of power and load voltage increase with decreasing pulse time.

These power and voltage levels are sufficient for performing periodic sensing and communication functions in a range of biomedical applications. It should be noted that the average power requirement for some applications can be minimised by varying the pulse width. For example, in cardiac pacing, it has been found that lower power is required for pulses of long duration with relatively low output voltage, rather than for pulses with shorter durations and commensurately higher output voltages (W E Hill 1988). Work is ongoing to demonstrate the coil performance in such applications.

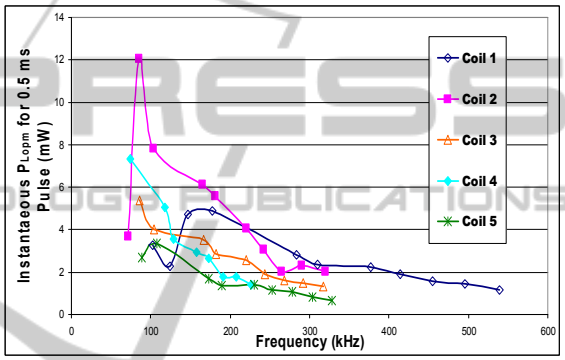

Figure 14: Maximum instantaneous power possible with in regulations for test coils for 0.50 ms pulse powering.

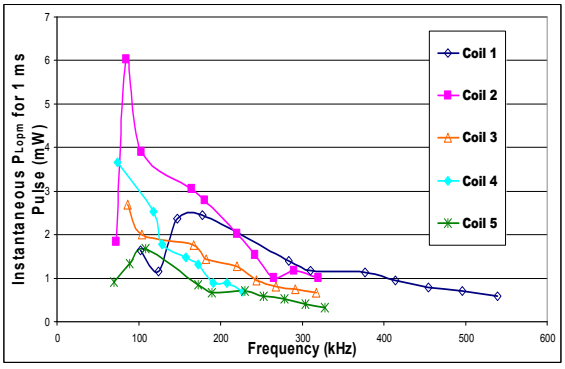

Figure 15: Maximum instantaneous power possible with in regulations for test coils for 1 ms pulse powering.

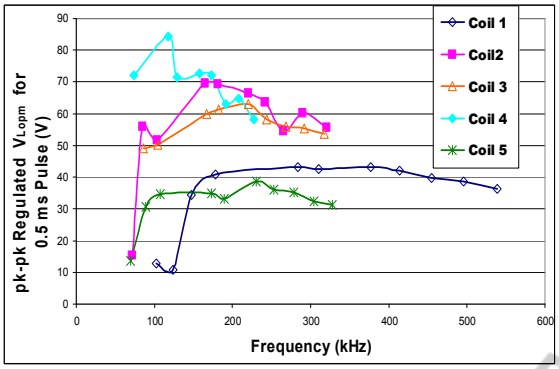

Figure 16: Peak-peak Load voltage possible for 0.5ms pulse powering.

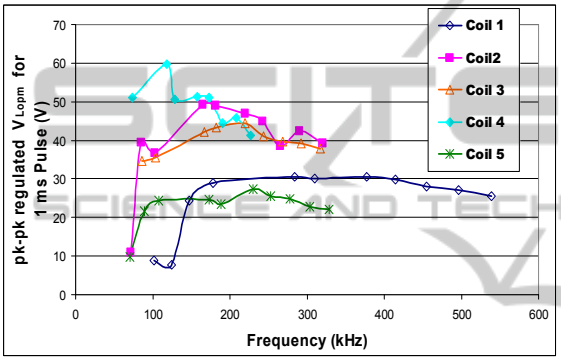

Figure 17: Peak-peak Load voltage possible for 1 ms pulse powering.

5 MEASUREMENTS

The five receiver coils were tested in the laboratory using a set-up as described by the circuit diagram in Figure 18. Each coil was measured for power transmission to a matched load for a range of frequencies. With the transmitter in a fixed position, the position of the receiver was set equal to 5.5 cm to make it comparable to a typical loosely coupled inductive implant. The function generator acts as a power supply feeding the transmitter coil through a parallel resonant tank, and a second resonant capacitor is connected across the receiver coil in parallel with a load resistor. A photograph of the test setup is shown in Figure 18a while its circuit diagram is shown in Figure 18b.

For each coil, the design procedure described in section 3.2 was used to determine values of the resonant capacitor and optimum load resistance for each test point. With the specified circuit values connected, a voltage of 20V pk-pk was applied from the function generator, and waveforms of pk-pk voltages across transmitter coil (CH 1) and matched load resistor (CH 4) were recorded. Note that a resonant capacitor was also applied on the transmitter side to compensate the high leakage inductance of the transmitter coil, thereby providing an enhanced transmitter coil current ($Q_1 I_{in}$), I_{tx} (CH 3). For example, results of transmitter coil and load resistance pk-pk voltages along with transmitter coil current are given for coil 3 at 167 kHz in Figure 19.

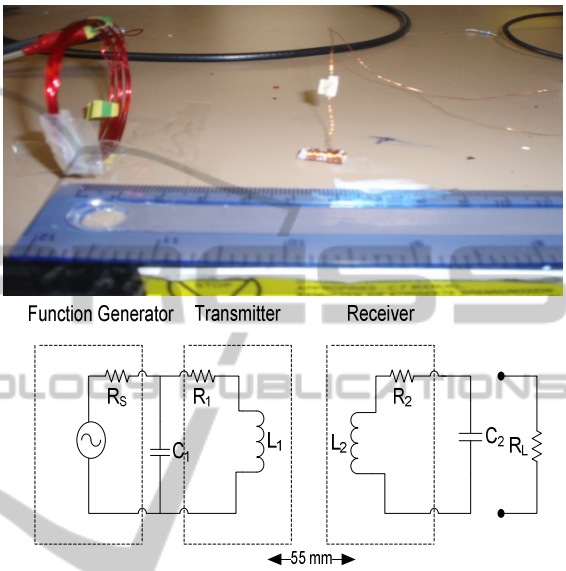

Figure 18: (a) Photograph (b) Circuit diagram of the inductive power system test set-up.

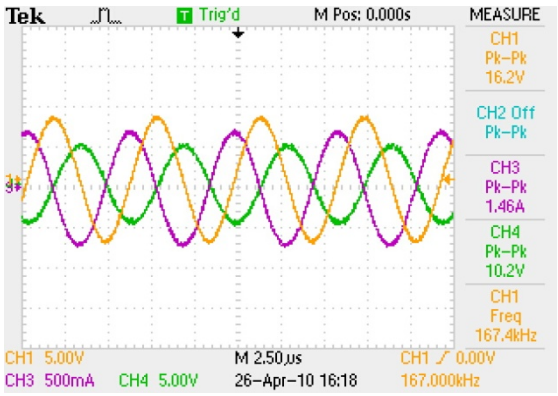

Figure 19: Measured transmitter coil and load voltage for coil 3 at 167 kHz.

To illustrate the low level of voltages induced on the receiver coils with no resonant capacitor included, measured values of open circuit pk-pk voltage induced on the receiver coils over the test frequency range according to the test setup in Figure 20 are shown in Figure 21.

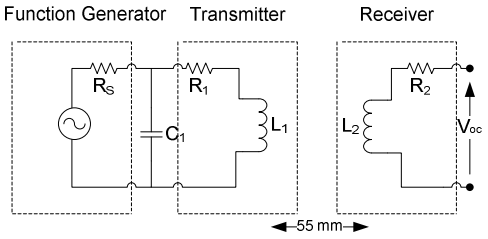

Figure 20: Measurement of open circuit induced voltage.

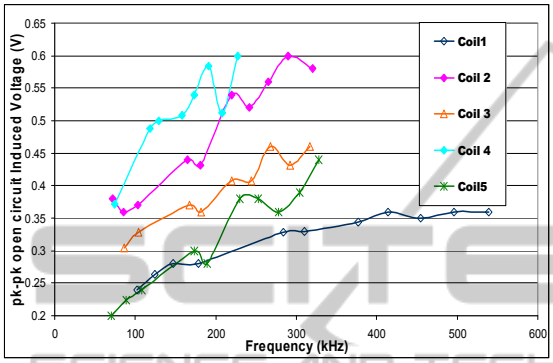

Figure 21: Measured pk-pk open circuit induced Voltages.

For comparison, theoretical (predicted according to (29)) and measured load voltages with a resonant capacitor included (according to test setup in Figure 18) are presented in Figure 22 for the five test coils over the frequency range from 100 – 600 kHz. In this case, the voltage source was set at 20 V pk-pk and the primary resonant capacitor was tuned so that the maximum current available was drawn from the supply for all measurement points.

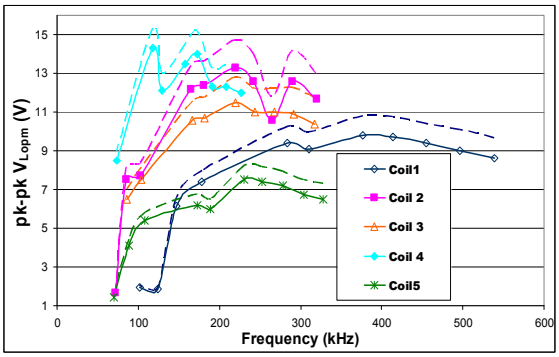

Figure 22: Theoretical (dashed) Vs Measured Load Voltages.

To validate the theoretical expression of maximum power transfer for the optimum load resistance, the results of load voltage were applied to predict corresponding values of load power in Figure 23.

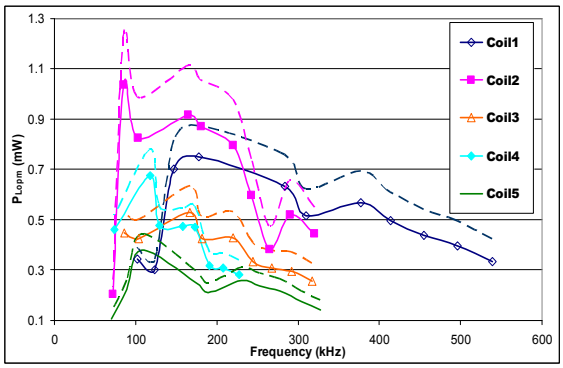

Figure 23: Predicted (dashed) vs. Measured continuous Power transfer to matched load.

The predicted and measured values of voltage and power match each other closely. However, there are deviations due to the unknown parasitic elements involved that have not been accounted for in the theoretical analysis. Moreover, it is impossible to compensate the transmitter and receiver coils fully because of the accuracy limitations of impedance measurements. The tolerances of capacitors, the self capacitance of the coils and the approximate values of the coil resistances at different frequencies cause deviations in the measured results. Nonetheless, the measurements confirm the trends in voltage and power levels predicted, and the same optimum receiver coil design is identified. Measurements of the continuous power scaled according to maximum field regulated current are shown in Figure 24, where again coil 2 is confirmed as the optimum design.

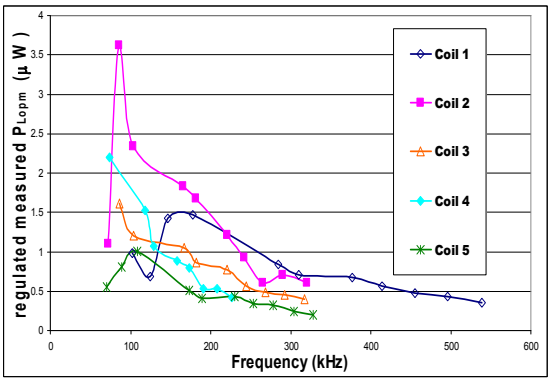

Figure 24: Measured continuous Power scaled according to field regulated transmitter current.

6 ANALYSIS & CONCLUSIONS

The design of an optimized receiver coil for providing sufficient power to a remote biomedical

implant within field regulations is the ultimate goal of this work. In order to determine this, five different coils were wound with different winding-core ratios and their behaviour was investigated at different frequencies. The performance of the system was determined through circuit design, analysis and experimentation. Practically, the transmitter coil was supplied with current from a function generator, where current levels were limited so that their associated magnetic fields were lower than specified by regulatory bodies. The receiver coil was placed at a distance (55 mm) from the transmitter coil, and voltage levels were measured under different operating frequencies.

The results of this work indicate that an optimum coil-core ratio for a certain receiver coil size is one in which the cross sectional area of the winding is approximately equal to that of the core. Average power levels of up to 4.3 μW are demonstrated within electromagnetic field regulations for a 5 mm diameter / 10 mm long receiver coil when located 55 mm from a transmitter coil. Pulsed power levels of up to 12 mW are illustrated.

Conditions for maximum power transfer are analyzed on the basis of matching the load with the receiver circuit impedance. It was found that there is significant variation in coil resistance with frequency and that this impacts on the maximum power that can be transmitted. The power transfer capability of each coil is illustrated in terms of the maximum power it can transmit to matched loads at different frequencies. Work is ongoing to customise the receiver and transmitter coil designs for specified load impedance values, which are typical of those encountered in biomedical applications. The impact of different core materials and wire dimensions will also be investigated both for the transmitter and receiver coils.

ACKNOWLEDGEMENTS

This work is supported by Enterprise Ireland and Brivant Ltd. under the Innovation Partnership Programme, Grant no. IP/2007/0447.

REFERENCES

Ahmadian, M., B. W. Flynn, et al. (2005). "Data transmission for implantable microsystems using magnetic coupling." communications, *IEEE proceedings*- 152(2): 247-250.

Ali, H., T. J. Ahmad, et al. (2009). Inductive link design for medical implants. Industrial electronics & applications, 2009. ISIEA 2009. *IEEE symposium*.

Atluri, S. And M. Ghovanloo (2005). Design of a wideband power-efficient inductive wireless link for implantable biomedical devices using multiple carriers. Neural engineering, 2005. *Conference proceedings. 2nd international IEEE EMBS conference.*

Clements, M., K. Vichienchom, et al. (1999). An implantable power and data receiver and neuro-stimulus chip for a retinal prosthesis system. Circuits and systems, 1999. *ISCAS '99. Proceedings of the 1999 IEEE international symposium*.

Djordje Popovic, l. L. B., and Gerald E. Loeb*, senior member, IEEE* (2007). "recruitment and comfort of Bion implanted electrical stimulation: implications for FES applications." *IEEE transactions on neural systems and rehabilitation engineering* 15(4).

Fair-rite. "fair-rite products corp. PO box J,One commercial row, Wallkill, NY 12589-0288", 2010, from www.fair-rite.com.

Flynn, K. F. A. B. W. Wireless powering of implanted sensors using RF inductive coupling.

Fotopoulou, K. And B. W. Flynn (2006). Wireless powering of implanted sensors using RF inductive coupling. Sensors, 2006. *5th IEEE conference*.

Furse, C. M., R. Harrison, et al. (2007). Recent advances in biomedical telemetry. Electromagnetics in advanced applications, 2007. *ICEAA 2007. International conference.*

Harrison, R., P. Watkins, et al. (2006). A low-power integrated circuit for a wireless 100-electrode neural recording system. Solid-state circuits conference, 2006. ISSCC 2006. Digest of technical papers. *IEEE international.*

Hmida, G. B., M. Dhieb, et al. (2006). Transcutaneous power and high data rate transmission for biomedical implants. Design and test of integrated systems in nanoscale technology, 2006. *DTIS 2006. International conference.*

IEEE standard. (1999). "IEEE standard for safety levels with respect to human exposure to radio frequency electromagnetic fields, 3 kHz to 300 GHz, 1999."

J. H. Schulman, J. P. M., J. Wolfe, E. Regev, C. Y. Perron, R. Ananth, E. Matei, A. Glukhovsky, R. Davis (2004). Battery powered Bion FES network. 26th annual international conference of the *IEEE EMBS San Francisco*, CA, USA.

Kihyun Jung, Y.-H. K., Euy Jung Choi, Hyun Jun Kim, and Yong-Jun Kim (2008). Wireless power transmission for implantable devices using inductive component of closed-magnetic circuit structure. *IEEE international conference on multisensor fusion and integration for intelligent systems*. Seoul, Korea.

Maxwell2d. "ansoft maxwell 2d." from www.ansoft.com.

Mounaim, F., M. Sawan, et al. (2009). Integrated inductive power and data recovery front-end dedicated to implantable devices. *Biomedical circuits and systems conference, 2009. BIOCAS 2009. IEEE*.

Noor, F. And M. Duffy (2009). Effect of a magnetic core in the receiver coil of a biomedical inductive power system. Engineering in medicine and biology society, 2009. *EMBC 2009. Annual international conference of the IEEE*.

Schuylenbergh, K., Puers, Robert (1999). Inductive powering , basic theory and application to biomedical systems.

Stielau, O. H. And G. A. Covic (2000). Design of loosely coupled inductive power transfer systems. Power system technology, 2000. *Proceedings. POWERCON 2000. International conference*.

W E Hill, A. M., J P Bourke, l Howell and R G Gold (1988). "Minimum energy for cardiac pacing." clinical physics and physiological measurement.

SCITEPRESS
SCIENCE AND TECHNOLOGY PUBLICATIONS